

Chapter 24

Compositional Variations in Palladium Electrodes Exposed to Electrolysis

A. Carpinteri, O. Borla, A. Goi, S. Guastella, A. Manuello, R. Sesana, and D. Veneziano

Abstract Literature presents several cases of nuclear anomalies occurring in condensed matter, during fracture of solids, cavitation of liquids, and electrolysis experiments.

Previous papers by the authors have recently shown that, on the surface of the electrodes exposed to electrolysis visible cracks and compositional changes are strictly related to nuclear particle emissions. In particular, a mechanical interpretation of the phenomenon was provided accounting to the hydrogen embrittlement effects. Piezonuclear reactions were considered responsible for the neutron and alpha particle emissions detected during the electrolysis. Such effects are thoroughly studied in a new experimental campaign, where three pure palladium (100 % Pd) cathodes coupled with Ni anodes are used for electrolysis, separately exposed to processes of different duration: 2.5 h, 5 h and 10 h, respectively. In this paper, the authors intend to show the new results concerning the changes on the surface of the electrodes in terms of composition and presence of cracks after the electrolytic process. Measures of heat generation as well as of neutron emission will be reported.

Keywords Hydrogen embrittlement • Cold fusion • Electrolysis • Piezonuclear reactions • Neutron emission • Energy balance

24.1 Introduction

Several evidences of anomalous nuclear reactions occurring in condensed matter were observed by different authors [1–34]. These experiments are characterized by extra heat generation, neutron emission, and alpha particle detection. Some of these studies, using electrolytic devices, reported also significant evidences of compositional variation after the microcracking of the electrodes. At the same time, recent experiments provided evidence of piezonuclear reactions occurring in condensed matter during fracture of solids, cavitation of liquids, and electrolysis experiments [35–40]. These experiments were characterized by significant neutron and alpha particle emissions, together with appreciable variations in the chemical composition. Based on these experimental evidences, a mechanical reason for the so-called Cold Nuclear Fusion was recently proposed by the same authors [41–43]. The hydrogen embrittlement due to H atoms produced by the electrolysis itself seems to play an essential role for the observed microcracking in the electrode host metals (Pd, Ni, Fe, etc.). Consequently, the hypothesis recently proposed is that piezonuclear fission reactions may occur in correspondence to the microcrack formation [41–45].

Classical experiments, belonging to the so called “Cold Fusion” research, are characterized by a generated heat several times greater than the input energy. In some cases, neutron emission rate, during electrolysis, was measured to be about three times the natural background level [6]. In 1998, Mizuno presented the results of the measurements conducted by means of neutron detectors and compositional analysis techniques related to different electrolytic experiments. According to Preparata, “despite the great amount of experimental results observed by a large number of scientists, a unified interpretation and theory of these phenomena has not been accepted and their comprehension still remains unsolved” [6–9, 26, 27].

A. Carpinteri (✉) • O. Borla • A. Manuello • D. Veneziano

Department of Structural, Geotechnical and Building Engineering, Politecnico di Torino, Corso Duca degli Abruzzi 24, Torino 10129, Italy
e-mail: alberto.carpinteri@polito.it; amedeo.manuellobertetto@polito.it

S. Guastella

Department of Applied Science and Technology, Geotechnical and Building Engineering, Politecnico di Torino, Corso Duca degli Abruzzi 24, Torino 10129, Italy

R. Sesana

Department of Mechanical and Aerospace Engineering, Politecnico di Torino, Corso Duca degli Abruzzi 24, Torino 10129, Italy

A. Goi

Private Research, Torino, Italy

On the other hand, as shown by most of the articles devoted to Cold Nuclear Fusion, one of the principal features is the appearance of microcracks on electrode surfaces after the tests [26, 27]. Such evidence might be directly correlated to hydrogen embrittlement of the material composing the metal electrodes (Pd, Ni, Fe, Ti, etc.). This phenomenon, well-known in Metallurgy and Fracture Mechanics, characterizes metals during forming or finishing operations [44]. In the present study, the host metal matrix (Pd and Ni) is subjected to mechanical damaging and fracturing due to hydrogen atoms penetrating into the atomic lattice and forcing it, during the gas loading. Hydrogen effects are largely studied especially in metal alloys where the hydrogen absorption is particularly high. The hydrogen atoms generate an internal stress that lowers the fracture resistance of the metal, so that brittle crack growth can occur with a hydrogen partial pressure below 1 atm [44, 45]. Some experimental evidences show that neutron emissions may be strictly correlated to fracture of non-radioactive or inert materials. From this point of view, anomalous nuclear emissions and heat generation had been verified during fracture in fissile materials [2–4] and in deuterated solids [5, 8, 30].

In order to confirm the earlier results obtained by Co–Cr and Ni–Fe electrodes [41, 42], and by Pd and Ni electrodes [43], electrolytic tests have been conducted using 100 % Pd at the cathode with different operating time intervals. As a result, relevant compositional changes and traces of elements previously absent have been observed on the Pd and Ni electrodes after the experiments and significant neutron emissions were observed during the test. In addition to the previous experimental campaign, also the amount of escaped gas during electrolysis was measured together with the evaluation of the extra heat generation during the tests in order to obtain an energy balance.

24.2 Experimental Set Up

Over the last ten years, specific experiments have been conducted on an electrolytic reactor (owners: Mr. A. Goi et al.). The aim was to investigate whether the anomalous heat generation may be correlated to a new type of nuclear reactions during electrolysis phenomena. The reactor was built in order to be appropriately filled with a salt solution of water and Potassium Carbonate (K_2CO_3). The electrolytic phenomenon was obtained using two metal electrodes immersed in the aqueous solution for three different tests of 2.5, 5 and 10 h (Fig. 24.1). The solution container, named also reaction chamber in the following, is a cylinder-shaped element of 100 mm diameter, 150 mm high, and 5 mm thick. For the reaction chamber Inox AISI 316 L steel was used. The two metallic electrodes were connected to a source of direct current: a Ni–Fe-based electrode as the positive pole (anode), and a Pd-based electrode as the negative pole (cathode).

The reaction chamber base consists of a ceramic plate preventing the direct contact between liquid solution and Teflon lid. Two threaded holes host the electrodes, which are screwed to the bottom of the chamber successively filled with the solution. A valve at the top of the cell allows the vapor to escape from the reactor and condense in an external collector. Externally, two circular Inox steel flanges, fastened by means of four threaded ties, hold the Teflon layers. The inferior steel flange of

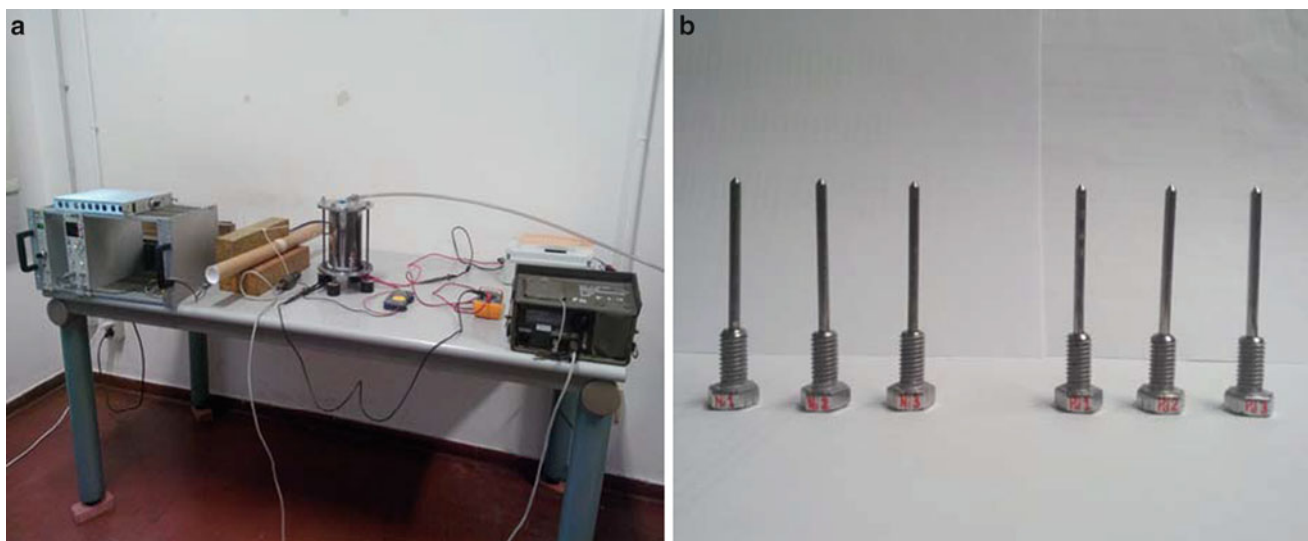


Fig. 24.1 Experimental set-up (a) Pd and Ni electrodes (b)

the reactor is connected to four supports isolated from the ground by means of rubber-based material. As mentioned before, a direct current passes through the anode and the cathode electrodes, provided by a power circuit connected to the power grid through an electric socket. The components of the circuit are an isolating transformer, an electronic variable transformer (Variac), and a diode bridge linked in series.

Electric current and voltage probes were positioned in different parts of the circuit. The voltage measurements were performed by a differential voltage probe of 100 MHz with a maximum rated voltage of 1400 V. The current was measured by a Fluke I 310S probe with a maximum rated current of 30 A. Current intensity and voltage measurements were also taken by means of a multimeter positioned at the input line. From the turning on to the switching off of the electrolytic cell, current and voltage were found to vary in a range from 3 to 5 A and from 20 to 120 V, respectively.

During testing an infrared thermo tracer IR Tech Timage Radimatic XT was placed in front of the specimens. A dedicated software, Timage Radimatic, allowed both acquisition and data processing. The equipment acquires a surface thermal contour of surfaces in front of the camera. Data are acquired as temperature data related to pixels and plotted by a colour map. Data processing procedure requires the definition of a ROI (Region of Interest) on the thermal map. The region can have any shape and dimension and it is possible to extract maximum, minimum, average and whatever temperature in the ROI. To optimize thermocamera measurement, reactor surface has been black painted, to minimize reflected radiation and maximize emitted radiation. The width of the area is of 20 pixels that is where the reactor surface can be approximated as parallel to the camera lens. In this ROI maximum, minimum and average temperature have been acquired with relation to time development. For what concerns temperature distribution in the reacting solution, the thermal map acquired by means of the thermo-camera shows convection streams during reaction taking place during reaction. Anyway the average temperature measured in the selected ROI shows a constant trend as long as maximum and minimum temperature trends in the same ROI. This allows us to assume the average temperature in the ROI equivalent to the average temperature in the solution.

For an accurate neutron emission evaluation, a He^3 proportional counter was employed (Xeram, France) with pre-amplification, amplification, and discrimination electronics directly connected to the detector tube. The detector is supplied by a high voltage power (about 1.3 kV) via NIM (Nuclear Instrument Module). The logic output producing the TTL (transistor–transistor logic) pulses is connected to a NIM counter. The logic output of the detector is enabled for analog signals exceeding 300 mV (see Fig. 24.1a). This discrimination threshold is a consequence of the sensitivity of the He^3 detector to the gamma rays ensuing neutron emission in ordinary nuclear processes. This value has been determined by measuring the analog signal of the detector by means of a Co-60 gamma source. The detector is also calibrated at the factory for the measurement of thermal neutrons; its sensitivity is 65 cps/ n_{thermal} ($\pm 10\%$ declared by the factory), i.e., the flux of thermal neutrons is one thermal neutron/s cm^2 , corresponding to a count rate of 65 cps. Finally, before and after the experiments, Energy Dispersive X-ray Spectroscopy has been performed in order to recognise possible direct evidence of piezonuclear reactions that can take place during the electrolysis. The elemental analyses were performed by a ZEISS Auriga field emission scanning electron microscope (FESEM) equipped with an Oxford INCA energy-dispersive X-ray detector (EDX) with a resolution of 124 eV @ MnKa. The energy used for the analyses was 18 KeV.

24.3 Neutron Emission Measurements

Neutron emission measurements performed during the experimental activity are represented in Figs. 24.2, 24.3 and 24.4. The measurements performed by the He^3 detector were conducted for different phases of 2.5, 5 and 10 h. The background level was measured for different time intervals before and after switching on the reaction chamber. These measurements reported an average neutron background of about $(6.00 \pm 2.45) \times 10^{-2}$ cps. Furthermore, when the reaction chamber is active, it is possible to observe that, after a time interval of about 80 min, neutron emissions greater than the background level may be detected in the first test (Fig. 24.2a). This evidence may be observed also in the cumulated curve of CPS respect to the cumulated average background level (Fig. 24.2b). During the experiment of 5 h After 260 min from the beginning of the measurements, it is possible to observe a neutron emission level of about 5 times greater than the background level (Fig. 24.3a). A small difference between the cumulated curves could be observed also in this case (Fig. 24.3b). Similar results were observed for the experiments of 10 h, after 200 min and up to 400 neutron emissions up to more than ten times the background were measured (Fig. 24.4a). This evidence may be observed also in the cumulated curve of CPS after 200 min from the beginning of the test (Fig. 24.4b).

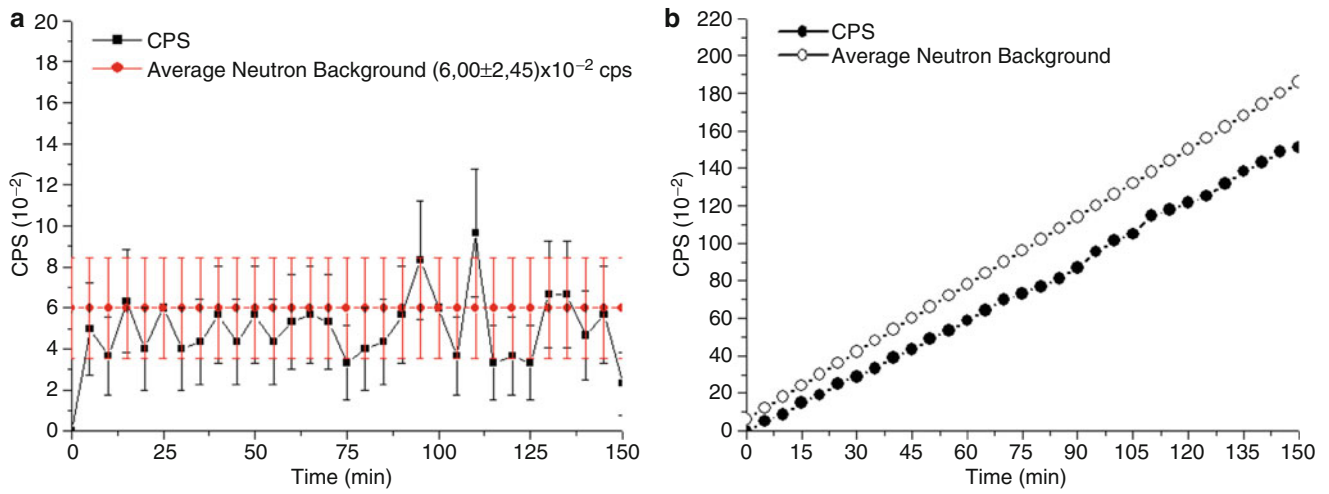


Fig. 24.2 Neutron emission measurements for the test with a time duration of 2.5 h (a). Cumulated curve of CPS respect to the cumulated average background level (b)

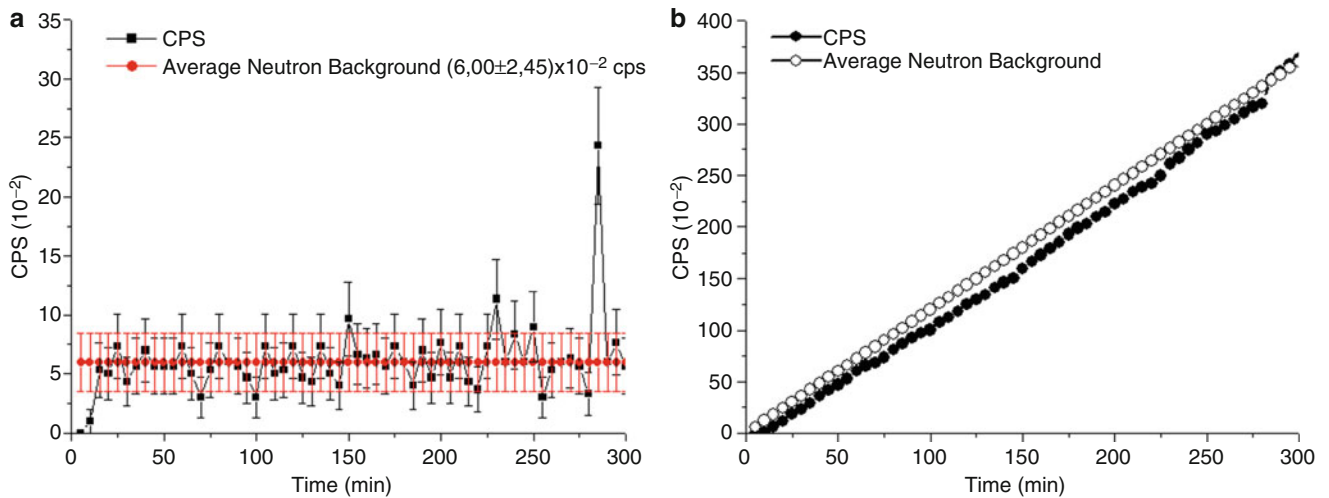


Fig. 24.3 Neutron emission measurements for the test with a time duration of 5 h (a). cumulated curve of CPS compared to the cumulated average background level (b)

24.4 Compositional Analysis of the PD Electrode

In the present section, the chemical compositions before and after the experiment will be taken into account (Fig.24.5a).

In particular, under the light of what can be deduced from the neutron emissions measurements and according to the hydrogen embrittlement hypothesis suggested by Carpinteri et al. [41–43], the presence of microcracks and macrocracks on the electrode surface (Fig. 24.5b) is accounted in the mechanical interpretation of the phenomena. These evidences are particularly strong in the case of the Pd electrode, where a macroscopic fracture took place during the test. The fracture presented a width of about 40 μm observable at naked eyes (see Fig. 24.5b).

Considering the average decrement of Pd (−28.9 %) after 10 h, reported in Table 24.1, according to the piezonuclear hypothesis a first fission reaction can be assumed:



according to reaction (24.1), a Pd decrement of about 2.07 % can be counterbalanced by the Zn and Si increments at the end of the experiment. reported in Table 24.1. By this reaction, in fact, increments of 1.46 % and 0.61 can be assumed for Zn

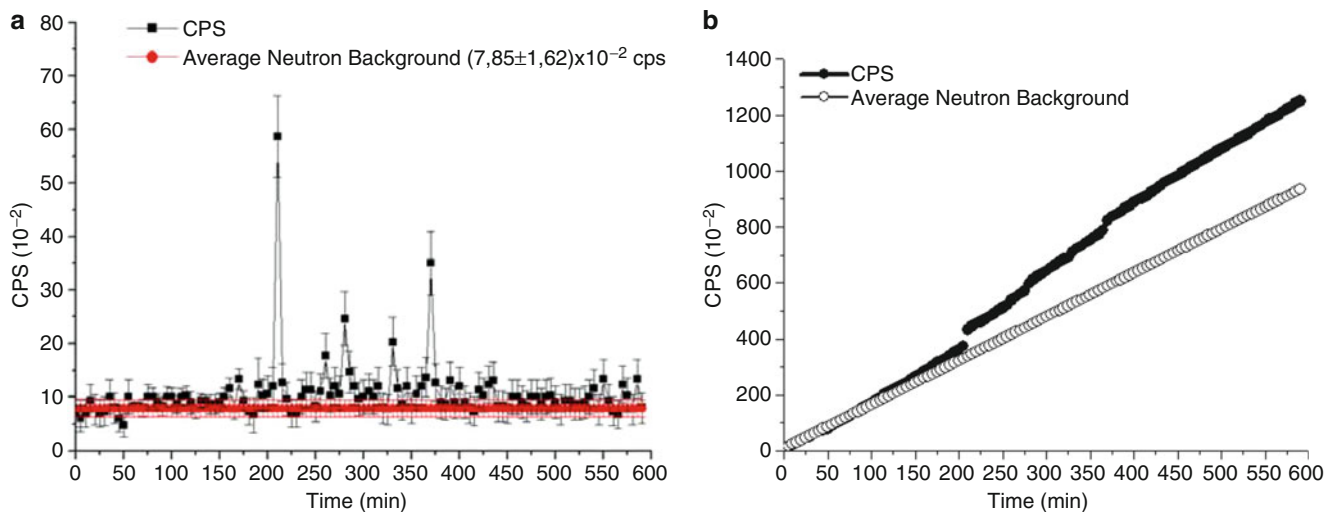


Fig. 24.4 Neutron emission measurements for the test with a time duration of 10 h (a); cumulated curve of CPS compared to the cumulated average background level (b)

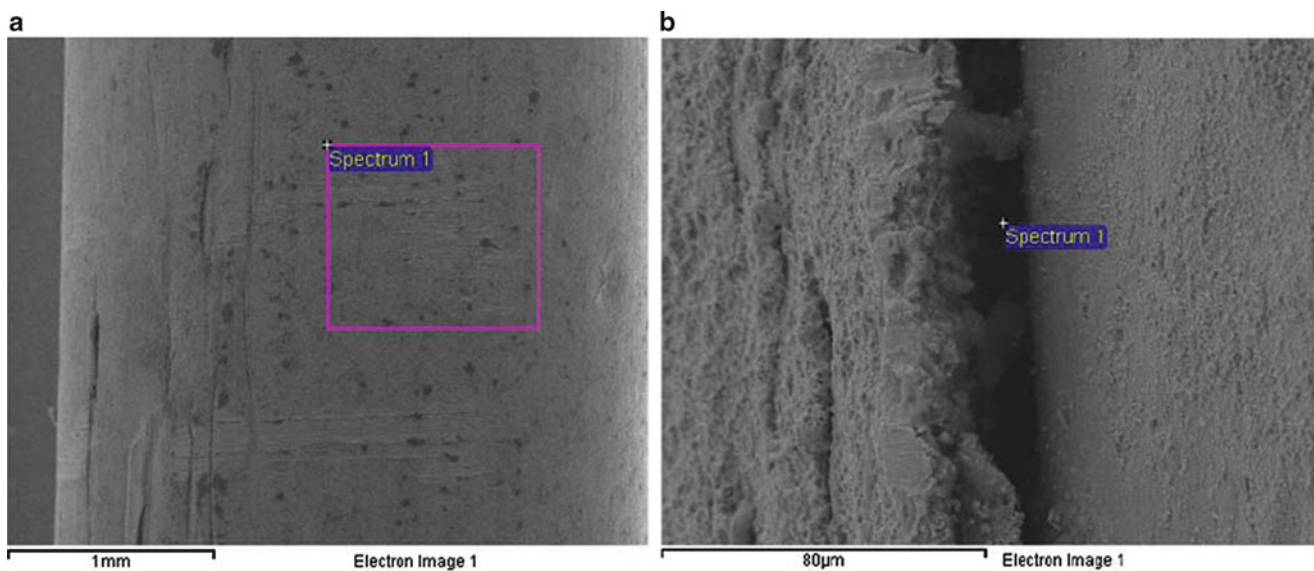


Fig. 24.5 Pd electrode; energy dispersive X-ray spectroscopy image before (a) and after (b) the test (10 h)

and Si, respectively. A quantity of 26.8 % of Pd remains to be counterbalanced. For these reasons, a second reaction can be assumed in analogy to previous experiments [43]:



Considering reaction (24.2), Ca and Fe respectively would increase by the following quantities: 10 % and 14 %. These variations may be accompanied by a neutron emission corresponding to the remaining 3 % of the mass concentration. The whole iron increment, according to reaction (24.2), could be entirely considered as the starting element for the production of other elements. Hence, a third hypothesis can be proposed involving Fe as starting element and O as the product, together with alpha and neutron emissions:



According to reaction (24.3), the iron depletion produces 11.9 % of oxygen with alpha particles (He) and neutron emissions. The total measured increment in oxygen after the experimental test is equal to 20.2 % (see Table 24.1). This

Table 24.1 Element concentrations before, after 2.5, 5 and 10 h of electrolysis (Pd electrode)

Element	Mean concentration (mass %)			
	0 h	2.5 h	5 h	10 h
Pd	99.85 ± 0.58	92.66 ± 3.42	88.26 ± 2.24	70.91 ± 4.63
O	0.15 ± 0.58	6.20 ± 2.89	9.04 ± 2.11	21.22 ± 3.64
K	–	0.41 ± 0.53	–	3.33 ± 0.86
Zn	–	–	–	1.46 ± 0.74
Fe	–	0.61 ± 0.61	2.67 ± 0.35	1.28 ± 0.45
Si	–	0.06 ± 0.17	–	0.61 ± 0.25
Mg	–	–	0.06 ± 0.2	0.42 ± 0.34
Na	–	0.06 ± 0, 22	–	0.29 ± 0.37
Cu	–	–	–	0.25 ± 0.67
Ni	–	–	–	0.11 ± 0.28
Ca	–	–	–	0.06 ± 0.23
Co	–	–	–	0.06 ± 0.24

Table 24.2 Element concentrations before, after 2.5, 5 and 10 h of electrolysis (Ni electrode)

Element	Mean concentration (mass %)			
	0 h	2.5 h	5 h	10 h
Ni	91.44 ± 0.86	76.57 ± 1.41	71.42 ± 2.43	72.66 ± 4.31
O	4.02 ± 0.70	18.52 ± 1.36	22.88 ± 2.08	16.97 ± 2.78
Pd	–	–	–	4.35 ± 1.12
Ti	3.43 ± 0.20	2.95 ± 0.16	2.77 ± 0.26	3.04 ± 0.25
Al	0.44 ± 0.13	0.89 ± 0.27	1.69 ± 0.23	1.57 ± 0.36
Si	0.67 ± 0.29	0.26 ± 0.27	0.50 ± 0.19	0.52 ± 0.08
Fe	–	0.03 ± 0.12	0.10 ± 0.21	0.31 ± 0.27
K	–	0.72 ± 0.16	0.64 ± 0.32	0.56 ± 0.35

quantity seems to be only partially explained by reaction (24.3). The remaining O concentration could be explained considering other reactions involving Ca (product in reaction 24.2) as the starting element:

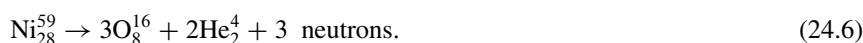


From reaction (24.4), we can consider a decrease in Ca concentration of 0.7 % and the formation of 0.42 % of Mg and 0.28 % of O. On the other hand, from reaction (24.5), we obtain a decrease in Ca corresponding to the increase of about 8 % in O with H production and neutron emissions. Considering the O increments coming from reactions (24.3), (24.4), and (24.5), totally equal to 19.9 %, and the experimental evidence reporting a total measured O concentration of 20.2 %, we may assume that O seems to be almost perfectly justified by the proposed reactions. At the same time, the Zn, Mg and Si increments observed after the experiment can be explained by the results of reactions (24.1) and (24.4). These evidences seem to be very interesting also considering that they represent a quantitative confirmation for the results previously published by Carpinteri et al. [43].

24.5 Nickel Electrode Composition Analysis

Analogously let us consider the Nickel electrode. Table 24.2 summarizes the concentration variations after the electrolysis. Nickel diminishes by 18.8 %, whereas the most apparent positive variation is that of oxygen (+12.9 %).

On the basis of the piezonuclear reaction conjecture, we could assume the oxygen average variation as a nuclear effect caused by the following hypothesis:



Reactions (24.6) and (24.7), imply emissions of neutrons and alpha particles, which will provide a great support to the hypotheses based on piezonuclear reactions. The main idea underlying the hypothesis is that an average decrease of 18.8 % in Nickel underwent a reaction producing at least 14.5 % of oxygen together with alpha and neutron emissions (3 %). Secondly, a further average depletion of 1.5 % in Ni would have produced about 1.3 % of Al accompanied by alpha particle emissions. According to reactions (24.6) and (24.7) the following balance: Ni (-18.8 %) = O (+14.5 %) + Al (+1.5 %) + neutrons and alpha particles may be considered. The amount of O coming from this balance (+14.5 %) and the amount detected after 10 h (+13 %) are very similar.

24.6 Heat Generation and Energy Balance Evaluation

The aim of the following considerations is to provide a thermodynamic background on the multiple phenomena involved in the energy equilibrium of the operating electrolytic cell. In particular, we shall define the physical quantities and the contributions required for an energy balance considering the input and output contributions. Thus, it is critical to define some hypotheses on the considered system. The input energy E_{in} is related to the electric power exchanged between the two electrodes and can be quantified by means of electric power consumption. The corresponding electric power ϕ_{in} can be calculated as the average power absorbed by the system and is given by direct electric measurements:

$$E_{in} = \frac{\int_{t_i}^{t_f} E_{in}(t) dt}{t_f - t_i}, \quad (24.8)$$

where t_f and t_i are the final and initial time instants respectively of the testing session. The instant input energy $E_{in}(t)$ is:

$$E_{in}(t) = V_{in} \times I(t), \quad (24.9)$$

where $V_{in}(t)$ is the measured voltage between the electrodes and $I(t)$ is the electric current intensity measured by means of the Amperometer placed before the cell, neglecting the circuit dissipations.

The main terms of energy transformation during testing are: (i) vaporization, and (ii) heat convection exchange. They are both “outgoing” power terms. The first term E_v can be computed by means of measuring the condensed water volume, as a pipe drives the exceeding vapour out of the reservoir, and its temperature while flowing in the pipe. The second term E_H can be quantified by means of thermodynamic heat exchange equations.

The energy equilibrium equation, involving the main energy terms, has the following formulation in steady state conditions:

$$E_{in} + E_X = E_v + E_H \quad (24.10)$$

Where E_{in} represents the term due to the power of the electric circuit, measured at the connection between the circuit and the electrodes just before the cell; E_X represents the unknown energy term correlated to piezonuclear reactions; E_v and E_H represent the terms due to vaporization and convection, respectively.

Other terms could be considered (electrolytic transformations, turbulent flow, etc.) but they are considered quantitatively negligible in a first approximation. According to (24.10), in a ten hour testing the input term counts by the electric measurers, neglecting the circuit dissipations, is 1349 kJ, the vaporization term counts 3953 kJ while the heat convection term is equal to 1460 kJ. The unbalance between the two terms of the equilibrium equation is about 4064 kJ, representing in a first approximation the estimation of the term E_X . The difference between output and input energies is about three times the input energy.

24.7 Conclusions

Neutron emissions up to one order of magnitude higher than the background level were observed during the operating time of an electrolytic cell. These evidences are very close to the results coming from previous experiments.

By the EDX analysis performed on the two electrodes, significant compositional variations were recorded. In general, the decrements in Pd at the first electrode seem to be almost perfectly counterbalanced by the increments in lighter elements

like oxygen, see reactions (24.1)–(24.5). As far as the Ni electrode is concerned, the Ni decrement is almost perfectly counterbalanced by the O and Al increments according to reactions (24.6) and (24.7).

The unbalance between the two terms of the thermal equilibrium equation is about 4064 kJ, representing in a first approximation the estimation of the energy production term. The amount E_x has been quantified as three times the input energy. Chemical variations, energy balance, and neutron emissions may be accounted for direct and indirect evidence of piezonuclear fission reactions correlated to microcrack formation and propagation as well as to hydrogen embrittlement. The so-called Cold Nuclear Fusion, interpreted under the light of hydrogen embrittlement, may be explained by piezonuclear fission reactions occurring in the host metal, rather than by nuclear fusion reactions of hydrogen isotopes forced by the atomic lattice.

Acknowledgement Special thanks for his collaboration in the realization of the tests are due to Mr. M. Yon.

References

- Borghi, D.C., Giori, D.C., Dall'Olio, A.: Experimental evidence on the emission of neutrons from cold hydrogen plasma. Proceedings of the International Workshop on Few-body Problems in Low-energy Physics, Alma-Ata, Kazakhstan, pp. 147–154 (1992); Unpublished Communication (1957); Comunicacao n. 25 do CENUFPE, Recife Brazil (1971)
- Diebner, K.: Fusionsprozesse mit Hilfe konvergenter Stosswellen—einige aeltere und neuere Versuche und Ueberlegungen. *Kerntechnik*. **3**, 89–93 (1962)
- Kaliski, S.: Bi-conical system of concentric explosive compression of D-T. *J. Tech. Phys.* **19**, 283–289 (1978)
- Winterberg, F.: Autocatalytic fusion–fission implosions. *Atomenergie-Kerntechnik*. **44**, 146 (1984)
- Derjaguin, B.V., et al.: Titanium fracture yields neutrons? *Nature* **34**, 492 (1989)
- Fleischmann, M., Pons, S., Hawkins, M.: Electrochemically induced nuclear fusion of deuterium. *J. Electroanal. Chem.* **261**, 301 (1989)
- Bockris, J.O'M., Lin, G.H., Kainthla, R.C., Packham, N.J.C., Velev, O.: Does tritium form at electrodes by nuclear reactions? In: The First Annual Conference on Cold Fusion. National Cold Fusion Institute, University of Utah Research Park, Salt Lake City (1990)
- Preparata, G.: Some theories of cold fusion: a review. *Fusion Technol.* **20**, 82 (1991)
- Preparata, G.: A new look at solid-state fractures, particle emissions and “cold” nuclear fusion. *Il Nuovo Cimento*. **104A**, 1259–1263 (1991)
- Mills, R.L., Kneizys, P.: Excess heat production by the electrolysis of an aqueous potassium carbonate electrolyte and the implications for cold fusion. *Fusion Technol.* **20**, 65 (1991)
- Notoya, R., Enyo, M.: Excess Heat Production during Electrolysis of H₂O on Ni, Au, Ag and Sn Electrodes in Alkaline Media, Proc. Third International Conference on Cold Fusion. Universal Academy Press, Tokyo (1992)
- Miles, M.H., Hollins, R.A., Bush, B.F., Lagowski, J.J., Miles, R.E.: Correlation of excess power and helium production during D₂O and H₂O electrolysis using palladium cathodes. *J. Electroanal. Chem.* **346**, 99–117 (1993)
- Bush, R.T., Eagleton, R.D.: Calorimetric studies for several light water electrolytic cells with nickel fibrex cathodes and electrolytes with alkali salts of potassium, rubidium, and cesium. In: Fourth International Conference on Cold Fusion. Lahaina, Maui. Electric Power Research Institute 3412 Hillview Ave., Palo Alto. (1993)
- Fleischmann, M., Pons, S., Preparata, G.: Possible theories of cold fusion. *Nuovo Cimento. Soc. Ital. Fis. A*. **107**, 143 (1994)
- Szpak, S., Mosier-Boss, P.A., Smith, J.J.: Deuterium uptake during Pd-D codeposition. *J. Electroanal. Chem.* **379**, 121 (1994)
- Sundaresan, R., Bockris, J.O.M.: Anomalous reactions during arcing between carbon rods in water. *Fusion Technol.* **26**, 261 (1994)
- Arata, Y., Zhang, Y.: Achievement of solid-state plasma fusion (“cold-fusion”). *Proc. Jpn Acad.* **71B**, 304–309 (1995)
- Ohmori, T., Mizuno, T., Enyo, M.: Isotopic distributions of heavy metal elements produced during the light water electrolysis on gold electrodes. *J. New Energy*. **1**(3), 90 (1996)
- Monti, R.A.: Low energy nuclear reactions: experimental evidence for the alpha extended model of the atom. *J. New Energy*. **1**(3), 131 (1996)
- Monti, R.A.: Nuclear transmutation processes of lead, silver, thorium, uranium. In: The Seventh International Conference on Cold Fusion. ENECO Inc. Vancouver (1998)
- Ohmori, T., Mizuno, T.: Strong excess energy evolution, new element production, and electromagnetic wave and/or neutron emission in light water electrolysis with a tungsten cathode. *Infinite Energy*. **20**, 14–17 (1998)
- Mizuno, T.: Nuclear Transmutation: The Reality of Cold Fusion. Infinite Energy Press, Concord (1998)
- Little, S.R., Puthoff, H.E., Little, M.E.: Search for Excess Heat from a Pt Electrode Discharge in K₂CO₃-H₂O and K₂CO₃-D₂O Electrolytes (1998)
- Ohmori, T., Mizuno, T.: Nuclear transmutation reaction caused by light water electrolysis on tungsten cathode under incandescent conditions. *Infinite Energy*. **5**(27), 34 (1999)
- Ransford, H.E.: Non-stellar nucleosynthesis: transition metal production by DC plasma-discharge electrolysis using carbon electrodes in a non-metallic cell. *Infinite Energy*. **4**(23), 16 (1999)
- Storms, E.: Excess power production from platinum cathodes using the Pons-Fleischmann effect. In: 8th International Conference on Cold Fusion. Lerici (La Spezia). Italian Physical Society, Bologna. pp. 55–61 (2000)
- Storms, E.: Science of Low Energy Nuclear Reaction: a Comprehensive Compilation of Evidence and Explanations about Cold Fusion. World Scientific, Singapore (2007)
- Mizuno, T., et al.: Production of heat during plasma electrolysis. *Jpn. J. Appl. Phys.* **39**, 6055–6061 (2000)
- Warner, J., Dash, J., Frantz, S.: Electrolysis of D₂O with titanium cathodes: enhancement of excess heat and further evidence of possible transmutation. In: The Ninth International Conference on Cold Fusion. Tsinghua University, Beijing, p. 404 (2002)

30. Fujii, M.F., et al.: Neutron emission from fracture of piezoelectric materials in deuterium atmosphere. *Jpn. J. Appl. Phys.* **41**, 2115–2119 (2002)
31. Mosier-Boss, P.A., et al.: Use of CR-39 in Pd/D co-deposition experiments. *Eur. Phys. J. Appl. Phys.* **40**, 293–303 (2007)
32. Swartz, M.: Three physical regions of anomalous activity in deuterated palladium. *Infinite Energy* **14**, 19–31 (2008)
33. Mosier-Boss, P.A., et al.: Comparison of Pd/D co-deposition and DT neutron generated triple tracks observed in CR-39 detectors. *Eur. Phys. J. Appl. Phys.* **51**(2), 20901–20911 (2010)
34. Kanarev, M., Mizuno, T.: Cold fusion by plasma electrolysis of water. *New Energy Technol.* **1**, 5–10 (2002)
35. Cardone, F., Mignani, R.: *Energy and Geometry*. World Scientific, Singapore (2004). Chapter 10
36. Carpinteri, A., Cardone, F., Lacidogna, G.: Piezonuclear neutrons from brittle fracture: early results of mechanical compression tests. *Strain.* **45**, 332–339 (2009). *Atti dell' Accademia delle Scienze di Torino.* **33**, 27–42 (2009)
37. Cardone, F., Carpinteri, A., Lacidogna, G.: Piezonuclear neutrons from fracturing of inert solids. *Phys. Lett. A.* **373**, 4158–4163 (2009)
38. Carpinteri, A., Cardone, F., Lacidogna, G.: Energy emissions from failure phenomena: mechanical, electromagnetic, nuclear. *Exp. Mech.* **50**, 1235–1243 (2010)
39. Carpinteri, A., Lacidogna, G., Manuello, A., Borla, O.: Piezonuclear fission reactions: evidences from microchemical analysis, neutron emission, and geological transformation. *Rock. Mech. Rock. Eng.* **45**, 445–459 (2012)
40. Carpinteri, A., Lacidogna, G., Manuello, A., Borla, O.: Piezonuclear fission reactions from earthquakes and brittle rocks failure: evidence of neutron emission and nonradioactive product elements. *Exp. Mech.* **53**, 345–365 (2013)
41. Carpinteri, A., Borla, O., Goi, A., Manuello, A., Veneziano, D.: Mechanical conjectures explaining cold nuclear fusion. *Proceedings of the Conference & Exposition on Experimental and Applied Mechanics (SEM), Lombard, CD-ROM*, p. 481 (2013)
42. Veneziano, D., Borla, O., Goi, A., Manuello, A., Carpinteri A.: Mechanical conjectures based on hydrogen embrittlement explaining cold nuclear fusion. *Proceedings of the 21° Congresso Nazionale di Meccanica Teorica ed Applicata (AIMETA), Torino, CD-ROM* (2013)
43. Carpinteri, A., Borla, O., Goi, A., Guastella, S., Manuello, A., Veneziano, D.: Hydrogen embrittlement and cold fusion effects in palladium during electrolysis experiments. In: *Conference & Exposition on Experimental and Applied Mechanics (SEM), Greenville, vol. 6, pp. 37–47* (2014)
44. Milne, I., Ritchie, R.O., Karihaloo, B.: *Comprehensive Structural Integrity: Fracture of Materials from Nano to Macro*, vol. 6, pp. 31–33. Elsevier, Amsterdam (2003)
45. Liebowitz, H.: *Fracture an Advanced Treatise*. Academic, New York (1971)